Bulk electronic structure of AV_3Sb_5 (A = K, Cs) studied by hard x-ray photoemission spectroscopy: Possibility of bond order without charge disproportionation

D. Takegami,[1,2] K. Fujinuma,[1] R. Nakamura,[1] M. Yoshimura,[3] K.-D. Tsuei,[3] N. L. Saini,[4] Zhiwei Wang,[5,6] Jia-Xin Yin,[7] and T. Mizokawa[1]

[1]*Department of Applied Physics, Waseda University, Tokyo 169-8555, Japan*
[2]*Max Planck Institute for Chemical Physics of Solids, 01187 Dresden, Germany*
[3]*National Synchrotron Radiation Research Center, 30076 Hsinchu, Taiwan*
[4]*Department of Physics, University of Roma "La Sapienza", Roma 00185, Italy*
[5]*Centre for Quantum Physics, Key Laboratory of Advanced Optoelectronic Quantum Architecture and Measurement (MOE), School of Physics, Beijing Institute of Technology, Beijing 100081, China*
[6]*Beijing Key Laboratory of Nanophotonics and Ultrafine Optoelectronic Systems, Beijing Institute of Technology, Beijing 100081, China*
[7]*Department of Physics, Southern University of Science and Technology, Shenzhen, Guangdong 518005, China*

(Received 22 December 2023; revised 13 February 2024; accepted 19 March 2024; published 2 April 2024)

The bulk electronic structure of AV_3Sb_5 (A = K, Cs) has been investigated by means of hard x-ray photoemission spectroscopy (HAXPES). The asymmetric shape of V and Sb core level peaks indicates that the V 3d and Sb 5p electrons are involved in the conduction band. The absence of a satellite structure in the V 2p HAXPES spectra shows a weak electronic correlation in the V 3d states. Splitting of the V 2p peak is not observed in the density wave phase indicating the charge disproportionation between the V sites is undetectably small, consistent with the weakness of the on-site electronic correlation and the possibility of bond order. The Sb $4d_{5/2}$ binding energy agrees with that of the Cs-terminated surface, indicating that the electronic structure of the V_3Sb_5 layer just below the Cs surface is close to the bulk.

DOI: 10.1103/PhysRevB.109.155108

I. INTRODUCTION

The interplay between the density wave and superconductivity in AV_3Sb_5 (A = K, Rb, Cs) with V kagome lattice layers has been attracting great interest in the condensed matter physics community [1–5] since their discovery by Ortiz *et al.* [1]. As shown in Fig. 1(a), the V ion is octahedrally coordinated by six Sb ions, two of which are located at the center of the V hexagon and four of which are located above and below the center of the V triangle of the kagome lattice illustrated in Fig. 1(b). The V 3d level is split into triply degenerate t_{2g} (xy, yz, and zx orbitals) and doubly degenerate e_g ($x^2 - y^2$ and $3z^2 - r^2$ orbitals) levels due to the cubic ligand field. Assuming K^+/Cs^+ and Sb^{3-}, the nominal valence of V is +4.67, and the V 3d t_{2g} orbitals accommodate 0.33 electrons per V site. In the density wave phase, the V kagome lattice undergoes a $2 \times 2 \times 2$ lattice distortion below ~78 K for KV_3Sb_5 and 94 K for CsV_3Sb_5 [7,8] probably due to charge modulation of the V 3d t_{2g} electrons. On the other hand, the multiband Fermi surfaces with imperfect Fermi-surface nesting are formed by V 3d and Sb 5p bands around the K point and Γ point of the hexagonal Brillouin zone, respectively, as revealed by angle-resolved photoemission spectroscopy [9–16]. Although the nature of the density wave has been studied by transport and optical measurements [17–21], its microscopic mechanism is still controversial. The orbital- and momentum-dependent energy gap at the Fermi level in the density wave phase [9–16] indicates that the Peierls mechanism due to the electron-lattice interaction alone may not be enough to explain the transition. Instead of the Fermi-surface instability, the van Hove singularities located at the M point around 0.1–0.2 eV below the Fermi level are found to show significant changes across the density wave transition [9–16]. The superconducting transition temperature is 0.93 K in KV_3Sb_5 and 2.5 K in CsV_3Sb_5 at ambient pressure [2–4]. The density wave is suppressed and the superconductivity is enhanced by pressure, suggesting that the density wave competes with the superconductivity [22–27]. In addition, the nematicity associated with the density wave and/or pair density wave manifests in the superconducting behavior [28–30].

In the $2 \times 2 \times 2$ lattice distortion with a star-of-David pattern, the V chains in the kagome layer have quadruple modulation. Taking the z axis along the in-plane V-Sb bond and the x and y axes along the out-of-plane V-Sb bonds, the lobes of the zx and yz orbitals roughly point to the neighboring V sites. If the V t_{2g} zx and yz orbitals accommodate 0.33 electrons per site, the zx and yz bands along the V chains in the kagome layer are 1/12 filling, which is inconsistent with the periodicity of the $2 \times 2 \times 2$ lattice distortion. However, the existence of the partially filled Sb 5p band suggests that the number of 3d electrons per V site is larger than 0.33. If the area of the unoccupied region of the Sb 5p band is approximately 85% of the Brillouin zone, $0.85 \times 2 = 1.7$ electrons are transferred to the three V sites. Then the number of 3d electrons per V site would be about 1.0, and the zx and yz bands along the V chains accommodate 0.5 electrons (1/4 filled), which is consistent with the quadruple modulation along the chains

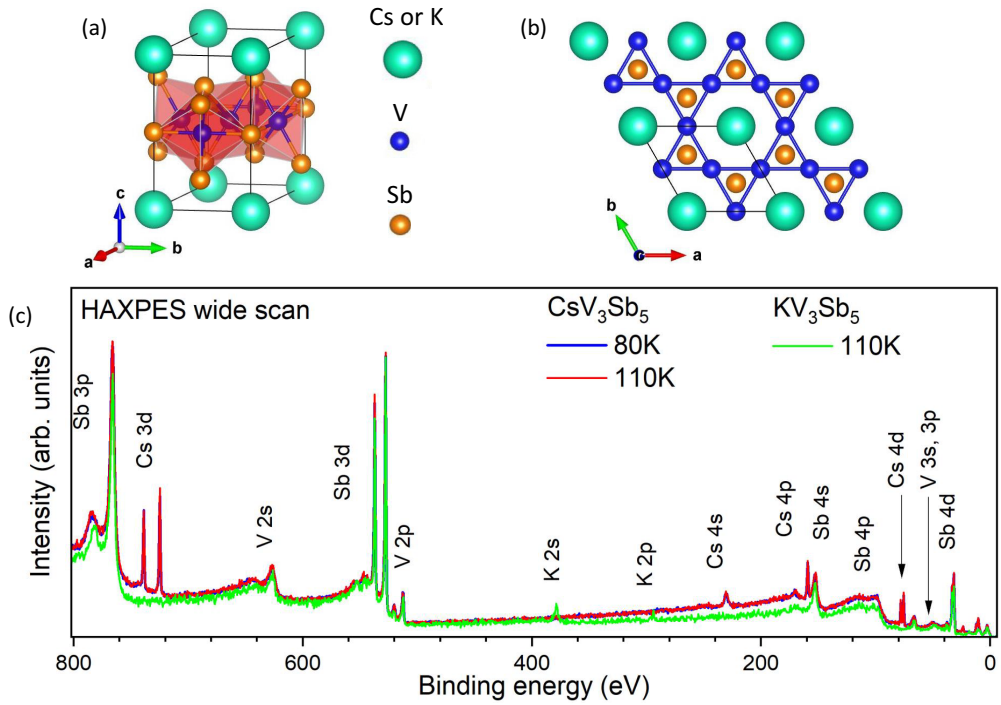

FIG. 1. (a) Crystal structure and (b) V kagome lattice of CsV_3Sb_5 and KV_3Sb_5 illustrated by VESTA [6]. The solid black lines and the shaded regions indicate the unit cell and the VSb_6 octahedra, respectively. (c) Wide scans taken at 80 and 110 K for CsV_3Sb_5 and taken at 110 K for KV_3Sb_5.

for the 2×2 density wave in the kagome lattice. However, such an orbital-dependent Peierls mechanism is insufficient to describe the three-dimensional $2 \times 2 \times 2$ density wave.

Nakayama *et al.* reported a momentum-dependent density wave gap which is enhanced around the M point and pointed out the importance of the van Hove singularities at the M points [9]. Kang *et al.* proposed that the k_z dependence of the van Hove singularities of the yz and zx bands (which are created by the mixing between the one-dimensional zx and yz bands described above) as well as those of the xy and $x^2 - y^2$ bands play essential roles in the $2 \times 2 \times 2$ density wave [10]. While the origin of the density wave can be assigned to the combination of the electron-electron interaction and the electron-lattice interaction, recent theoretical works assume that the driving force is the electronic interaction enhanced by the van Hove singularities [31–35]. Denner, Thomale, and Neupert showed that bond order without charge disproportionation is stabilized relative to the charge density order with charge disproportionation for $U/V < 2.1$ (U and V are on-site and intersite electron-electron Coulomb interactions in the extended Hubbard model) [32]. However, the effect of electronic correlation is not clear in the existing experimental results. As for the pairing mechanism of the superconductivity, an electronic interaction such as spin and/or orbital fluctuations is proposed to play essential roles [31,33].

The angle-resolved photoemission spectroscopy (ARPES) studies have been playing central roles in identifying the nature of the density wave. However, the reported values of the density-wave-driven energy gap as well as their momentum dependence differ among the literature [9–14]. The strong momentum dependence of the energy gap makes it difficult to evaluate its magnitude by means of scanning tunneling spectroscopy [22] and optical spectroscopy [20]. In the surface-sensitive ARPES studies of CsV_3Sb_5, the energy gap (the separation between the peak and the hump) is observed to be ∼50 meV by Kato *et al.* [14] while it is ∼30 meV in the study by Lou *et al.* [13]. On the other hand, in the optical study, spectral weight up to ∼80 meV is suppressed in the density wave phase, suggesting a larger energy gap [20]. The apparent inconsistency between the ARPES and optical studies suggests that the electronic structure of the surface region is different from the bulk. In addition, the microfocused ARPES work on CsV_3Sb_5 revealed that the ARPES results are significantly different between the Cs-terminated and Sb-terminated surfaces [14]. In this context, it is highly important to investigate the fundamental electronic structure of AV_3Sb_5 by means of a bulk-sensitive technique such as hard x-ray photoemission spectroscopy (HAXPES). In the present paper, we perform systematic HAXPES measurements on CsV_3Sb_5 and KV_3Sb_5. The V $2p$ HAXPES spectra indicate a weak electronic correlation of the V $3d$ electrons and the absence of V charge disproportionation in the density wave state of CsV_3Sb_5.

II. METHODS

CsV_3Sb_5 and KV_3Sb_5 crystals were grown as reported in the literature [3]. HAXPES was performed at the Max-Planck-NSRRC HAXPES endstation with the MB Scientific A-1 HE analyzer, Taiwan undulator beamline BL12XU of SPring-8 [36]. The photon energy was set to 6.5 keV that has a probing depth of about 10 nm. The x-ray incidence angle was about 15°, and the photoelectron detection angle was 90°. The radius of the beam spot was about 50 μm. The

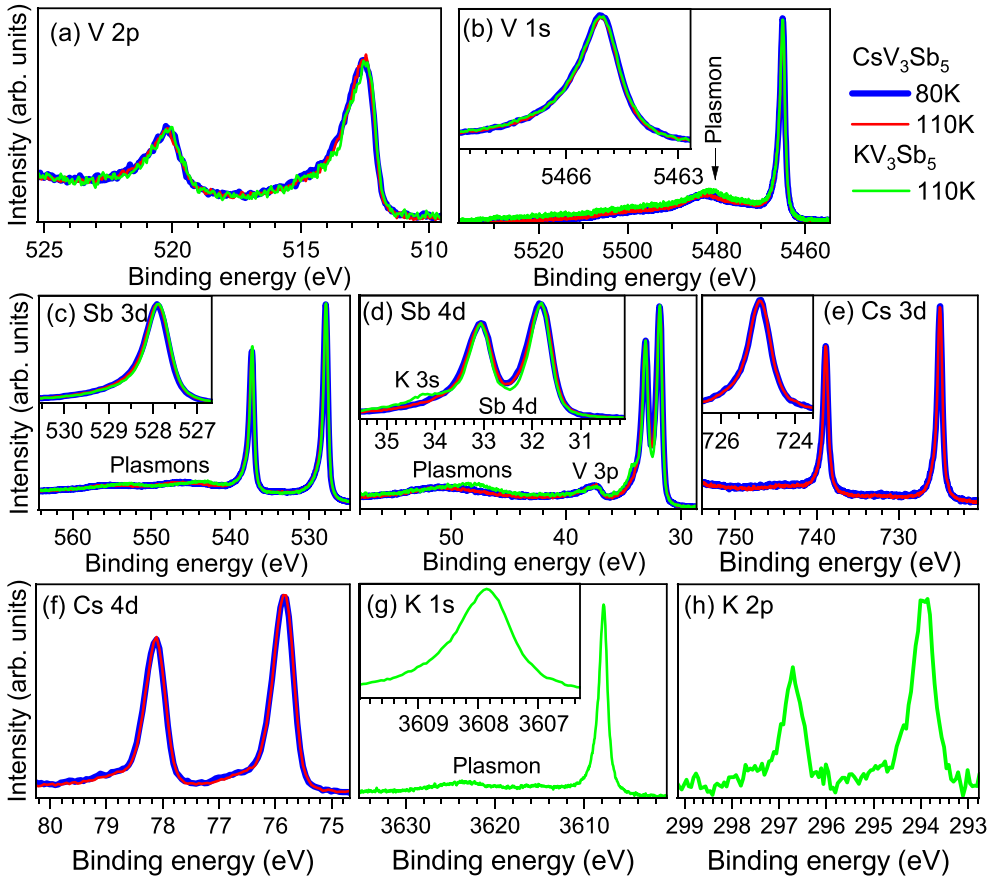

FIG. 2. (a) V 2*p*, (b) V 1*s*, (c) Sb 3*d*, and (d) Sb 4*d* HAXPES spectra taken at 80 and 110 K for CsV_3Sb_5 and taken at 110 K for KV_3Sb_5. (e) Cs 3*d* and (f) Cs 4*d* HAXPES spectra taken at 80 and 110 K for CsV_3Sb_5. (g) K 1*s* and (h) K 2*p* HAXPES spectra taken at 110 K for KV_3Sb_5.

crystals were cleaved under an ultrahigh vacuum of 10^{-6} Pa at room temperature in order to avoid surface contamination. The measurements were performed at 80 and 110 K. The binding energy of the HAXPES spectra was calibrated using the Fermi edge of Au. The total energy resolution estimated from the Fermi edge was about 300 meV.

To compute the total and partial (i.e., orbitally resolved) single particle density of states (DOS and PDOS), density functional theory calculations within the local density approximation (LDA) using the full-potential local-orbital code (FPLO version 21.00-61) [37] was employed using the exchange and correlation potential of Perdew and Wang and a four-component full-relativistic, nonmagnetic approach. For the Brillouin zone integration, we used the tetrahedron method with a $12 \times 12 \times 12$ k mesh. The experimental crystal structure parameters as reported in Ref. [1] were used for the calculations. Except for the crystal structure parameters from the studied compounds [1], and the full-relativistic settings, for all other settings including the numerics, k mesh, basis functions, etc., the default input settings from FPLO version 21.00-61 were used [37].

III. RESULTS AND DISCUSSION

Wide scans for CsV_3Sb_5 and KV_3Sb_5 taken at 80 and 110 K are displayed in Fig. 1(c). All observed features correspond to core level peaks of V, Sb, and Cs/K as expected from the sample composition. In particular, the lack of a C and O signal indicates the cleanliness and lack of oxidation in the measured surface. As for KV_3Sb_5, K 2*s* and 2*p* core level peaks are observed in addition to the Sb and V core levels in rough agreement with the composition. Figure 2(a) shows V 2*p* HAXPES spectra for CsV_3Sb_5 taken at 80 and 110 K and for KV_3Sb_5 taken at 110 K. V $2p_{3/2}$ and V $2p_{1/2}$ peaks exhibit asymmetric shapes with tails on the higher binding energy side. The asymmetric shape corresponds to the Mahan line shape or Doniach-Šunjić line shape due to electron-hole excitations in the V 3*d* conduction bands. The difference between 80 and 110 K is not appreciable in CsV_3Sb_5, indicating that the electronic structure change induced by the density wave is limited to the small energy scale compared to the energy resolution of 0.3 eV. The negligibly small impact of the density wave on the core level spectra is in sharp contrast to the significant impact of the charge density wave in transition-metal chalcogenides such as TaS_2 [38] and $IrTe_2$ [39]. The situation of CsV_3Sb_5 is similar to that of VS_2 with a charge density wave in which the V 2*p* line shape indicates a weak on-site electronic correlation and has no signature of charge disproportionation [40]. The V 2*p* HAXPES spectra of KV_3Sb_5 are similar to those of CsV_3Sb_5. The binding energy of the V 2*p* peaks is about 512.5 eV, which is lower than that of VS_2 with V^{4+} around 515 eV [40] and is comparable to those of

V^{2+} oxides around 513 eV [41,42]. It should be noted that, with the energy resolution of ∼300 meV, differences in the peak positions of the order of at least ∼50 meV can still be reliably determined. The binding energy shift indicates a substantial amount of charge transfer from Sb 5*p* to V 3*d*. Here, one can speculate that the amount of charge transfer is varied by applying pressure, and the position of the van Hove singularities relative to the Fermi level can be tuned. Figure 2(b) shows V 1*s* HAXPES spectra for CsV_3Sb_5 taken at 80 and 110 K and for KV_3Sb_5 taken at 110 K. While the main peaks do not show any appreciable change between 80 and 110 K as well as between Cs and K, the energy loss peak due to the valence plasmon is shifted to the higher binding energy in going from K to Cs. The valence plasmon energy increases from about 15 eV for KV_3Sb_5 to about 18 eV for CsV_3Sb_5 due to the participation of Cs 5*p* electrons to the valence plasmon.

As shown in Figs. 2(c) and 2(d), Sb 3*d* and 4*d* peaks are asymmetric with tails on the higher binding energy side due to the electron-hole excitation at the Fermi level. The binding energy of the Sb $3d_{5/2}$ peaks is about 528 eV which is comparable to that of the Sb metal [43]. These observations are consistent with the participation of the Sb 5*p* orbitals to the conduction band. The Cs 3*d* and 4*d* core level peaks in Figs. 2(e) and 2(f) and the K 1*s* and 2*p* core level peaks in Figs. 2(g) and 2(h) are more symmetric that the V and Sb core level peaks. The Cs and K core level peaks still exhibit weak asymmetry with a tail on the higher binding energy side indicating that the outer shells of Cs 6*s* and K 4*s* are involved in the conduction bands. The microfocused ARPES study by Kato *et al.* revealed that the binding energy of Cs $4d_{5/2}$ is about 75.9 and 76.8 eV for the Sb-terminated and Cs-terminated surfaces, respectively [14]. In the bulk-sensitive HAXPES, the Cs $4d_{5/2}$ peak is located at 75.9 eV which is close to that of the Sb-terminated surface. On the other hand, the Sb $4d_{5/2}$ peak is located at 31.8 eV which is rather close to that of the Cs-terminated surface although the energy difference between the Cs- and Sb-terminated surfaces is as small as 0.13 eV [14]. This observation indicates that the electronic structure of the V_3Sb_5 layer just below the top Cs layer is close to that of the bulk. This is consistent with the fact that the band folding and the energy gap are observed by ARPES only in the Cs-terminated surface.

Figure 3(a) shows valence-band HAXPES spectra taken at 80 and 110 K for CsV_3Sb_5 and taken at 110 K for KV_3Sb_5. The Cs $5p_{3/2}$ and $5p_{1/2}$ peaks are located around 11.5 and 13.5 eV, respectively, and partially overlap with the broad Sb 5*s* band ranging from 7 to 13 eV. These assignments are supported by the LDA calculations displayed in Fig. 3(b). The difference in the valence-band spectra between 80 and 110 K is negligibly small in CsV_3Sb_5 although a density wave gap is expected to open around 95 K. The absence of the energy gap at 80 K is apparently inconsistent with the optical study by Zhou *et al.* in which the large optical gap ∼70 meV develops well already around 80 K [20]. However, at the present excitation energy (about 6.5 keV), the spectral weight near the Fermi level is dominated by the Sb 5*p* contribution due to the effect of the photoionization cross section [44] as shown in Fig. 3(c). While the optical gap is governed by the V 3*d* orbitals, the HAXPES spectral weight probes the Sb 5*p* orbitals forming the Fermi surface around the Γ point.

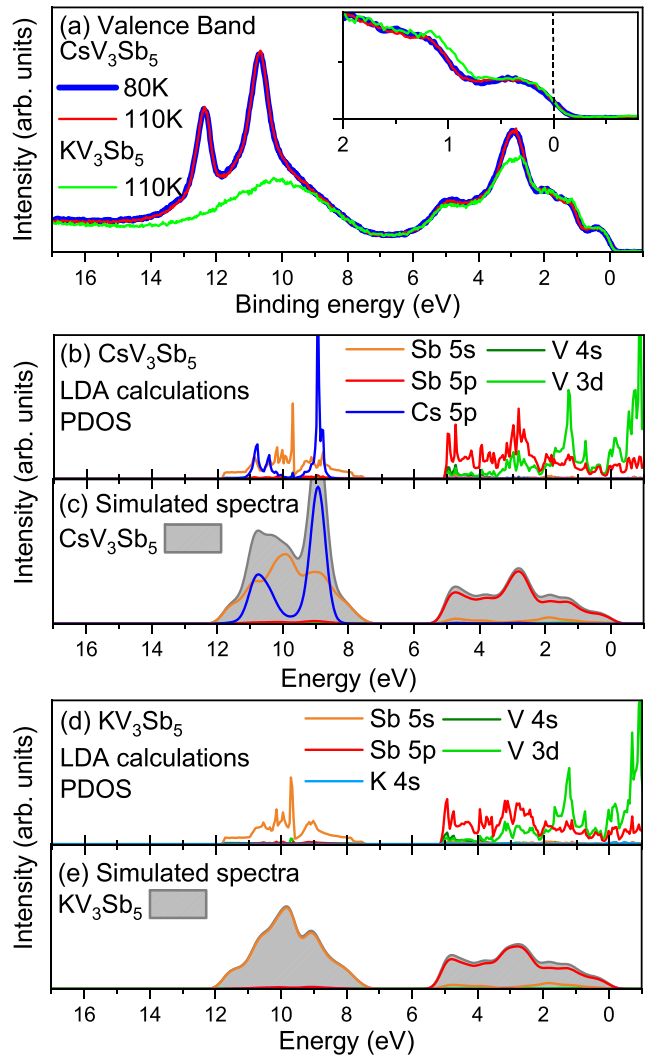

FIG. 3. (a) Valence-band HAXPES spectra taken at 80 and 110 K for CsV_3Sb_5 and taken at 110 K for KV_3Sb_5. (b) DOS and PDOS calculated for CsV_3Sb_5 within LDA using the full-potential local-orbital code [37], and (c) simulated spectra obtained from the PDOS and the photoionization cross sections of the atomic orbitals [44]. (d) DOS and PDOS calculated for KV_3Sb_5 and (e) simulated spectra obtained from the PDOS and the photoionization cross sections.

Calculated partial densities of states for CsV_3Sb_5 are shown in Fig. 3(b). The calculations produce a metallic solution with very wide V 3*d* and Sb 5*p* bands crossing the Fermi level consistent with previously reported results in the literature [34,35]. We note that the binding energy of the Cs 5*p* semicore level is underestimated in the calculations, but otherwise the calculated features are in good agreement with the experimental spectra. The partial densities of states are multiplied by photoionization cross sections for each atomic subshell [44] and the obtained results are shown in Fig. 3(c). The valence-band spectral shape is well reproduced by the simulated one which is mainly derived from the Sb 5*s* and 5*p* contribution. Calculated partial densities of states for KV_3Sb_5 are shown in Fig. 3(d). The weak but finite contribution of K

4*s* existing near the Fermi level is consistent with the asymmetric phase of the K core level peaks. The partial densities of states are multiplied by photoionization cross sections for each atomic subshell and the obtained results are shown in Fig. 3(e). The broadening of the peak around 3 eV in the experimental result of KV_3Sb_5 is well reproduced by the simulation. The excellent agreement between the valence-band HAXPES spectra and the simulated spectra based on the band calculation shows that the electronic correlation is very weak at least for the Sb 5*s* and 5*p* electrons.

The V 2*p* HAXPES results indicate that the on-site electronic correlation of the V 3*d* electrons in AV_3Sb_5 (A = K, Cs) is rather weak. It would be comparable to or even weaker than that of VS_2 [40]. In addition, the V charge disproportionation is not detected in the V 2*p* core level peak both in AV_3Sb_5 and in VS_2. In VS_2 and VSe_2, the charge density wave is driven by partial Fermi-surface nesting and the electron-lattice interaction [45–47]. Here, one can speculate that the driving force of the density wave in AV_3Sb_5 (A = K, Cs) is also the electron-lattice interaction. On the other hand, the electron-lattice interaction alone is not enough to stabilize the density wave with time-reversal symmetry breaking which is experimentally observed in KV_3Sb_5 [3,5,17]. Indeed, we cannot exclude the possibility that the effect of the remaining electron-electron interaction is enhanced by the flat band at the van Hove singularities to provide the time-reversal symmetry breaking as theoretically predicted in the extended Hubbard models [32,33]. The present HAXPES results show that the on-site electron-electron interaction U is well screened, suggesting a small U/V ratio. Although the well-screened electron-electron interaction alone may not be enough to trigger the density wave at about 100 K, a collaboration with the electron-lattice interaction may stabilize the bond order theoretically predicted for small U/V [32]. The bond order without charge disproportionation is indeed consistent with the V 2*p* core level spectra.

IV. CONCLUSION

In conclusion, the HAXPES measurements on AV_3Sb_5 (A = K, Cs) revealed highly asymmetric V and Sb core level peaks, indicating their highly metallic character and the involvement of the V 3*d* and Sb 5*p* electrons in the conduction band. The Sb $4d_{5/2}$ binding energy of the bulk agrees with that of the Cs-terminated surface [14], indicating that the electronic structure of the V_3Sb_5 layer just below the Cs surface is close to the bulk. The absence of a satellite structure in the V 2*p* spectra, as well as the good agreement of band-structure calculations with the valence-band spectra, shows that the on-site electronic correlations are very weak in the highly metallic V 3*d* states. Furthermore, the binding energies of the V 2*p* and Sb 3*d* core levels indicate a substantial amount of charge transfer from Sb to V. Splitting of the V 2*p* peak is not observed in the density wave phase, indicating charge disproportionation between the V sites is undetectably small, consistent with the weakness of the electronic correlation and the possibility of the bond order. These observations suggest that the density wave is mainly driven by the electron-lattice interaction.

ACKNOWLEDGMENTS

D.T. acknowledges the support by the Deutsche Forschungsgemeinschaft (DFG, German Research Foundation) under the Walter Benjamin Programme, Projektnummer 521584902. J.-G.C. thanks the support from the National Natural Science Foundation of China (Grants No. 12025408 and No. 11921004), and the National Key R&D Program of China (Grant No. 2021YFA1400200). We acknowledge the support for the measurements from the Max Planck-POSTECH-Hsinchu Center for Complex Phase Materials. This work was partially supported by Grants-in-Aid from JSPS (Grant No. JP22H01172).

[1] B. R. Ortiz, L. C. Gomes, J. R. Morey, M. Winiarski, M. Bordelon, J. S. Mangum, I. W. H. Oswald, J. A. Rodriguez-Rivera, J. R. Neilson, S. D. Wilson, E. Ertekin, T. M. McQueen, and E. S. Toberer, New kagome prototype materials: discovery of KV_3Sb_5, RbV_3Sb_5, and CsV_3Sb_5, Phys. Rev. Mater. **3**, 094407 (2019).

[2] B. R. Ortiz, S. M. L. Teicher, Y. Hu, J. L. Zuo, P. M. Sarte, E. C. Schueller, A. M. M. Abeykoon, M. J. Krogstad, S. Rosenkranz, R. Osborn, R. Seshadri, L. Balents, J. He, and S. D. Wilson, CsV_3Sb_5: A $\mathbb{Z}_2$ topological kagome metal with a superconducting ground state, Phys. Rev. Lett. **125**, 247002 (2020).

[3] Y.-X. Jiang, J.-X. Yin, M. M. Denner, N. Shumiya, B. R. Ortiz, G. Xu, Z. Guguchia, J. He, M. S. Hossain, X. Liu, J. Ruff, L. Kautzsch, S. S. Zhang, G. Chang, I. Belopolski, Q. Zhang, T. A. Cochran, D. Multer, M. Litskevich, Z.-J. Cheng *et al.*, Unconventional chiral charge order in kagome superconductor KV_3Sb_5, Nat. Mater. **20**, 1353 (2021).

[4] B. R. Ortiz, P. M. Sarte, E. M. Kenney, M. J. Graf, S. M. L. Teicher, R. Seshadri, and S. D. Wilson, Superconductivity in the $\mathbb{Z}_2$ kagome metal KV_3Sb_5, Phys. Rev. Mater. **5**, 034801 (2021).

[5] J.-X. Yin, B. Lian, and M. Z. Hasan, Topological kagome magnets and superconductors, Nature (London) **612**, 647 (2022).

[6] K. Momma and F. Izumi, *VESTA* 3 for three-dimensional visualization of crystal, volumetric and morphology data, J. Appl. Crystallogr. **44**, 1272 (2011).

[7] Z. Liang, X. Hou, F. Zhang, W. Ma, P. Wu, Z. Zhang, F. Yu, J.-J. Ying, K. Jiang, L. Shan, Z. Wang, and X.-H. Chen, Three-dimensional charge density wave and robust zero-bias conductance peak inside the superconducting vortex core of a kagome superconductor CsV_3Sb_5, Phys. Rev. X **11**, 031026 (2021).

[8] H. X. Li, T. T. Zhang, T. Yilmaz, Y. Y. Pai, C. E. Marvinney, A. Said, Q. W. Yin, C. S. Gong, Z. J. Tu, E. Vescovo, C. S. Nelson, R. G. Moore, S. Murakami, H. C. Lei, H. N. Lee, B. J. Lawrie, and H. Miao, Observation of unconventional charge density wave without acoustic phonon anomaly in kagome superconductors AV_3Sb_5 (A = Rb, Cs), Phys. Rev. X **11**, 031050 (2021).

[9] K. Nakayama, Y. Li, T. Kato, M. Liu, Z. Wang, T. Takahashi, Y. Yao, and T. Sato, Multiple energy scales and anisotropic

energy gap in the charge-density-wave phase of the kagome superconductor CsV_3Sb_5, Phys. Rev. B **104**, L161112 (2021).

[10] M. Kang, S. Fang, J.-K. Kim, B. R. Ortiz, S. H. Ryu, J. Kim, J. Yoo, G. Sangiovanni, D. D. Sante, B.-G. Park, C. Jozwiak, A. Bostwick, E. Rotenberg, E. Kaxiras, S. D. Wilson, J.-H. Park, and R. Comin, Twofold van Hove singularity and origin of charge order in topological kagome superconductor CsV_3Sb_5, Nat. Phys. **18**, 301 (2022).

[11] Z. Liu, N. Zhao, Q. Yin, C. Gong, Z. Tu, M. Li, W. Song, Z. Liu, D. Shen, Y. Huang, K. Liu, H. C. Lei, and S.-C. Wang, Observation of unconventional charge density wave without acoustic phonon anomaly in kagome superconductors AV_3Sb_5 ($A =$ Rb, Cs), Phys. Rev. X **11**, 041010 (2021).

[12] S. Cho, H. Ma, W. Xia, Y. Yang, Z. Liu, Z. Huang, Z. Jiang, X. Lu, J. Liu, Z. Liu, J. Li, J. Wang, Y. Liu, J. Jia, Y. Guo, J. Liu, and D. W. Shen, Emergence of new van Hove singularities in the charge density wave state of a topological kagome metal RbV_3Sb_5, Phys. Rev. Lett. **127**, 236401 (2021).

[13] R. Lou, A. Fedorov, Q. Yin, A. Kuibarov, Z. Tu, C. Gong, E. F. Schwier, B. Büchner, H. Lei, and S. Borisenko, Charge-density-wave-induced peak-dip-hump structure and the multiband superconductivity in a kagome superconductor CsV_3Sb_5, Phys. Rev. Lett. **128**, 036402 (2022).

[14] T. Kato, Y. Li, K. Nakayama, Z. Wang, S. Souma, M. Kitamura, K. Horiba, H. Kumigashira, T. Takahashi, and T. Sato, Polarity-dependent charge density wave in the kagome superconductor CsV_3Sb_5, Phys. Rev. B **106**, L121112 (2022).

[15] T. Kato, Y. Li, T. Kawakami, M. Liu, K. Nakayama, Z. Wang, A. Moriya, K. Tanaka, T. Takahashi, Y. Yao, and T. Sato, Three-dimensional energy gap and origin of charge-density wave in kagome superconductor KV_3Sb_5, Commun. Mater. **3**, 30 (2022).

[16] Y. Hu, X. Wu, B. R. Ortiz, S. Ju, X. Han, J. Ma, N. C. Plumb, M. Radovic, R. Thomale, S. D. Wilson, A. P. Schnyder, and M. Shi, Rich nature of Van Hove singularities in Kagome superconductor CsV_3Sb_5, Nat. Commun. **13**, 2220 (2022).

[17] F. H. Yu, T. Wu, Z. Y. Wang, B. Lei, W. Z. Zhuo, J. J. Ying, and X. H. Chen, Concurrence of anomalous Hall effect and charge density wave in a superconducting topological kagome metal, Phys. Rev. B **104**, L041103 (2021).

[18] H. Zhao, H. Li, B. R. Ortiz, S. M. L. Teicher, T. Park, M. X. Ye, Z. Q. Wang, L. Balents, S. D. Wilson, and I. Zeljkovic, Cascade of correlated electron states in a kagome superconductor CsV_3Sb_5, Nature (London) **599**, 216 (2021).

[19] H. Chen, H. Yang, B. Hu, Z. Zhao, J. Yuan, Y. Xing, G. Qian, Z. Huang, G. Li, Y. Ye, S. Ma, S. Ni, H. Zhang, Q. Yin, C. Gong, Z. Tu, H. Lei, H. Tan, S. Zhou, C. Shen *et al.*, Roton pair density wave in a strong-coupling kagome superconductor, Nature (London) **599**, 222 (2021).

[20] X. Zhou, Y. Li, X. Fan, J. Hao, Y. Dai, Z. Wang, Y. Yao, and H.-H. Wen, Origin of charge density wave in the kagome metal CsV_3Sb_5 as revealed by optical spectroscopy, Phys. Rev. B **104**, L041101 (2021).

[21] Z. X. Wang, Q. Wu, Q. W. Yin, C. S. Gong, Z. J. Tu, T. Lin, Q. M. Liu, L. Y. Shi, S. J. Zhang, D. Wu, H. C. Lei, T. Dong, and N. L. Wang, Unconventional charge density wave and photoinduced lattice symmetry change in the kagome metal CsV_3Sb_5 probed by time-resolved spectroscopy, Phys. Rev. B **104**, 165110 (2021).

[22] Q. Wang, P. Kong, W. Shi, C. Pei, C. Wen, L. Gao, Y. Zhao, Q. Yin, Y. Wu, G. Li, H. Lei, J. Li, Y. Chen, S. Yan, and Y. Qi, Charge density wave orders and enhanced superconductivity under pressure in the kagome metal CsV_3Sb_5, Adv. Mater. **33**, 2102813 (2021).

[23] Z. Zhang, Z. Chen, Y. Zhou, Y. Yuan, S. Wang, J. Wang, H. Yang, C. An, L. Zhang, X. Zhu, Y. Zhou, X. Chen, J. Zhou, and Z. Yang, Pressure-induced reemergence of superconductivity in the topological kagome metal CsV_3Sb_5, Phys. Rev. B **103**, 224513 (2021).

[24] F. H. Yu, D. H. Ma, W. Z. Zhuo, S. Q. Liu, X. K. Wen, B. Lei, J. J. Ying, and X. H. Chen, Unusual competition of superconductivity and charge-density-wave state in a compressed topological kagome metal, Nat. Commun. **12**, 3645 (2021).

[25] T. Qian, M. H. Christensen, C. Hu, A. Saha, B. M. Andersen, R. M. Fernandes, T. Birol, and N. Ni, Revealing the competition between charge density wave and superconductivity in CsV_3Sb_5 through uniaxial strain, Phys. Rev. B **104**, 144506 (2021).

[26] C. C. Zhu, X. F. Yang, W. Xia, Q. W. Yin, L. S. Wang, C. C. Zhao, D. Z. Dai, C. P. Tu, B. Q. Song, Z. C. Tao, Z. J. Tu, C. S. Gong, H. C. Lei, Y. F. Guo, and S. Y. Li, Double-dome superconductivity under pressure in the V-based kagome metals AV_3Sb_5 ($A =$ Rb and K), Phys. Rev. B **105**, 094507 (2022).

[27] H. S. Xu, Y. J. Yan, R. Yin, W. Xia, S. Fang, Z. Chen, Y. Li, W. Yang, Y. Guo, and D. L. Feng, Multiband superconductivity with sign-preserving order parameter in kagome superconductor CsV_3Sb_5, Phys. Rev. Lett. **127**, 187004 (2021).

[28] Y. Xiang, Q. Li, Y. Li, W. Xie, H. Yang, Z. Wang, Y. Yao, and H.-H. Wen, Twofold symmetry of c-axis resistivity in topological kagome superconductor CsV_3Sb_5 with in-plane rotating magnetic field, Nat. Commun. **12**, 6727 (2021).

[29] D. Wulferding, S. Lee, Y. Choi, Q. Yin, Z. Tu, C. Gong, H. Lei, and K.-Y. Choi, Emergent nematicity and intrinsic versus extrinsic electronic scattering processes in the kagome metal CsV_3Sb_5, Phys. Rev. Res. **4**, 023215 (2022).

[30] D. Song, L. Zheng, F. Yu, J. Li, L. Nie, M. Shan, D. Zhao, S. Li, B. Kang, Z. Wu, Y. Zhou, K. Sun, K. Liu, X. Luo, Z. Wang, J. Ying, X. Wan, T. Wu, and X. Chen, Orbital ordering and fluctuations in a kagome superconductor CsV_3Sb_5, Sci. China: Phys., Mech. Astron. **65**, 247462 (2022).

[31] H. X. Tan, Y. Liu, Z. Wang, and B. H. Yan, Charge density waves and electronic properties of superconducting kagome metals, Phys. Rev. Lett. **127**, 046401 (2021).

[32] M. M. Denner, R. Thomale, and T. Neupert, Analysis of charge order in the kagome metal AV_3Sb_5 ($A =$ K, Rb, Cs), Phys. Rev. Lett. **127**, 217601 (2021).

[33] R. Tazai, Y. Yamakawa, S. Onari, and H. Kontani, Mechanism of exotic density-wave and beyond-Migdal unconventional superconductivity in kagome metal AV_3Sb_5 ($A =$ K, Rb, Cs), Sci. Adv. **8**, eabl4108 (2022).

[34] H. LaBollita and A. S. Botana, Tuning the van Hove singularities in AV_3Sb_5 ($A =$ K, Rb, Cs) via pressure and doping, Phys. Rev. B **104**, 205129 (2021).

[35] A. Subedi, Hexagonal-to-base-centered-orthorhombic 4Q charge density wave order in kagome metals KV_3Sb_5, RbV_3Sb_5, and CsV_3Sb_5, Phys. Rev. Mater. **6**, 015001 (2022).

[36] J. Weinen, T. C. Koethe, C. F. Chang, S. Agrestini, D. Kasinathan, Y. F. Liao, H. Fujiwara, C. Schler-Langeheine,

F. Strigari, T. Haupricht, G. Panaccione, F. Offi, G. Monaco, S. Huotari, K.-D. Tsuei, and L. H. Tjeng, Polarization dependent hard X-ray photoemission experiments for solids: Efficiency and limits for unraveling the orbital character of the valence band, J. Electron Spectrosc. Relat. Phenom. **198**, 6 (2015).

[37] K. Koepernik and H. Eschrig, Full-potential nonorthogonal local-orbital minimum-basis band-structure scheme, Phys. Rev. B **59**, 1743 (1999); https://www.fplo.de/.

[38] S. Hellmann, M. Beye, C. Sohrt, T. Rohwer, F. Sorgenfrei, H. Redlin, M. Kalläne, M. Marczynski-Bühlow, F. Hennies, M. Bauer, A. Föhlisch, L. Kipp, W. Wurth, and K. Rossnagel, Ultrafast melting of a charge-density wave in the Mott insulator $1T$-TaS_2, Phys. Rev. Lett. **105**, 187401 (2010).

[39] D. Ootsuki, Y. Wakisaka, S. Pyon, K. Kudo, M. Nohara, M. Arita, H. Anzai, H. Namatame, M. Taniguchi, N. L. Saini, and T. Mizokawa, Orbital degeneracy and Peierls instability in the triangular-lattice superconductor $Ir_{1-x}Pt_xTe_2$, Phys. Rev. B **86**, 014519 (2012).

[40] M. Mulazzi, A. Chainani, N. Katayama, R. Eguchi, M. Matsunami, H. Ohashi, Y. Senba, M. Nohara, M. Uchida, H. Takagi, and S. Shin, Absence of nesting in the charge-density-wave system $1T$-VS_2 as seen by photoelectron spectroscopy, Phys. Rev. B **82**, 075130 (2010).

[41] T. Yoshino, M. Okawa, T. Kajita, S. Dash, R. Shimoyama, K. Takahashi, Y. Takahashi, R. Takayanagi, T. Saitoh, D. Ootsuki, T. Yoshida, E. Ikenaga, N. L. Saini, T. Katsufuji, and T. Mizokawa, Unusual valence state and metal-insulator transition in $BaV_{10}O_{15}$ probed by hard x-ray photoemission spectroscopy, Phys. Rev. B **95**, 075151 (2017).

[42] D. Takegami, T. Miyoshino, A. Melendez-Sans, R. Nakamura, M. Ferreira-Carvalho, G. Poelchen, M. Yoshimura, K.-D. Tsuei, A. Tanaka, H. Matsumoto, A. Yanagida, R. Yoshimura, T. Katsufuji, L. H. Tjeng, and T. Mizokawa (unpublished).

[43] D. J. Morgan, Metallic antimony (Sb) by XPS, Surf. Sci. Spectra **24**, 024004 (2017).

[44] M. B. Trzhaskovskaya and V. G. Yarzhemsky, Dirac-Fock photoionization parameters for HAXPES applications, At. Data Nucl. Data Tables **119**, 99 (2018).

[45] S.-H. Lee, Y. C. Park, J. Chae, G. Kim, H. J. Kim, B. K. Choi, I. H. Lee, Y. J. Chang, S.-H. Chun, M. Jung, J. Seo, and S. Lee, Strong electron-phonon coupling driven charge density wave states in stoichiometric $1T$-VS_2 crystals, J. Mater. Chem. C **10**, 16657 (2022).

[46] V. N. Strocov, M. Shi, M. Kobayashi, C. Monney, X. Wang, J. Krempasky, T. Schmitt, L. Patthey, H. Berger, and P. Blaha, Three-dimensional electron realm in VSe_2 by soft-x-ray photoelectron spectroscopy: Origin of charge-density waves, Phys. Rev. Lett. **109**, 086401 (2012).

[47] P. Chen, W. W. Pai, Y.-H. Chan, V. Madhavan, M. Y. Chou, S.-K. Mo, A.-V. Fedorov, and T.-C. Chiang, Unique gap structure and symmetry of the charge density wave in single-layer VSe_2, Phys. Rev. Lett. **121**, 196402 (2018).